Constituents of *Polygala flavescens* ssp. *flavescens* and Their Activity as Inhibitors of Human Lactate Dehydrogenase

Marinella De Leo,[†] Lorenzo Peruzzi,[‡,§] Carlotta Granchi,[†] Tiziano Tuccinardi,[†,§] Filippo Minutolo,[†,§] Nunziatina De Tommasi,*[⊥] and Alessandra Braca[†,§]

[†]Dipartimento di Farmacia, Università di Pisa, via Bonanno 6 and 33, 56126 Pisa, Italy

[‡]Dipartimento di Biologia, Università di Pisa, via Derna 1, 56126 Pisa, Italy

[§]Centro Interdipartimentale di Ricerca "Nutraceutica e Alimentazione per la Salute", Università di Pisa, via del Borghetto 80, 56124 Pisa, Italy

[⊥]Dipartimento di Farmacia, Università degli Studi di Salerno, via Giovanni Paolo II 132, 84084 Fisciano (SA), Italy

ABSTRACT: Four new flavonol glycosides (**1-4**), two oligosaccharides (**5-6**), one α-ionone (**7**), and three triterpenoid saponins (**8-10**), together with four known secondary metabolites (**11-14**), were isolated from the aerial parts of *Polygala flavescens* ssp. *flavescens*. All structures were elucidated on the basis of their spectroscopic and spectrometric data. The isolates were assayed for their inhibitory activity against isoform 5 of human lactate dehydrogenase and compound **11** (3,6'-di-*O*-sinapoylsucrose) showed an IC_{50} value of 90.4 µM. Modeling studies were carried out to suggest the putative interaction mode of compound **11** in the enzyme active site.

Polygala L. is the largest genus of the Polygalaceae, comprising about 500 species (about half of the entire family), including trees, shrubs, and herbs distributed throughout the world except New Zealand and the Arctic.[1] Some species are used in folk medicine for their content of triterpenoid saponins,[2] but the genus is also well-known for producing several classes of secondary metabolites, such as xanthones, oligosaccharides, lignans, and other phenolic compounds.[2-4] Recently, interest in the genus has increased since only a relatively small number of the known species have been chemically and biologically explored. In Italy, the genus *Polygala* includes only herbs, with fourteen specific and subspecific taxa endemic to the country.[5,6] Among these *Polygala flavescens* DC. is the only Italian species with yellow flowers, with a geographical distribution ranging from Liguria to Basilicata, across the Italian peninsula. To the best of our knowledge, all of the Italian *Polygala* species have been investigated minimally so far.

In the course of a research program on the lactate dehydrogenase (LDH) inhibitory activity of different classes of natural products,[7,8] *P. flavescens* ssp. *flavescens* was selected as the subject of this investigation. The human isoform 5 of the enzyme lactate dehydrogenase (*h*LDH5, composed of four A subunits), which is overexpressed in many types of invasive tumors, catalyses the final step of glycolysis, the reduction of pyruvate to lactate, thus playing a key role in cancer cell metabolism. *h*LDH5 allows energy production in tumor cells, which largely depend on aerobic glycolysis for their growth and survival and exhibit high glucose uptake together with an increased lactate production.[9] Therefore, *h*LDH5 inhibition should cause cancer cell death by starvation, without interfering with healthy cells that normally use oxidative phosphorylation for ATP generation. So far, several LDH inhibitors have been reported in the literature[10] and, in particular, some of them are derived from natural sources.[11,12] Therefore, the search for natural *h*LDH5 inhibitors represents an attractive goal to find new effective anticancer drugs and prompted the present investigation. A chemical study of *P. flavescens* ssp. *flavescens* led to the isolation and structural characterization of ten new compounds, including four flavonol glycosides (**1-4**), two oligosaccharides (**5** and **6**), an α-ionone (**7**), and three triterpenoid saponins (**8-10**), together with

four known secondary metabolites constituted by two oligosaccharide (**11** and **12**) and two flavonol glycosides (**13** and **14**). The isolates were assayed for their LDH inhibitory activity.

RESULTS AND DISCUSSION

The aerial parts of *P. flavescens* subsp. *flavescens* were defatted with *n*-hexane and extracted with methanol to afford a MeOH extract, which was partitioned between AcOEt, *n*-BuOH, and H_2O to give a *n*-BuOH residue. This extract was subjected to size exclusion and RP-HPLC separations to afford ten new (**1-10**) and four known compounds (**11-14**).

Compound **1**, a yellow amorphous solid, showed a sodiated molecular ion peak at *m/z* 869.2102 for $[M + Na]^+$ in the HRESIMS; this result, together with the ^{13}C NMR data, allowed the assignment of the molecular formula $C_{39}H_{42}O_{21}$ to **1**. In the ESIMS, fragments obtained in the negative mode at *m/z* 723 $[M - H - 122]^-$ and 591 $[M - H - 122 - 132]^-$ and in the positive mode at *m/z* 723 $[M + Na - 146]^+$ revealed the presence of a benzoyl moiety along with one pentose and one deoxyhexose residue each in the molecule. The UV spectrum of **1** showed two absorption maxima at 260 and 356 nm, indicating the presence of a flavonol derivative. The ^1H and ^{13}C NMR spectra of compound **1** (Table 1) showed a typical pattern of a quercetin aglycone, with signals ascribable to sugar moieties and to a benzoyl residue.[13,14] Three sugar residues having anomeric protons at δ 4.50 (d, $J = 1.8$ Hz), 5.52 (d, $J = 3.0$ Hz) and 5.60 (d, $J = 7.5$ Hz), which correlated, respectively, with signals at δ 102.1, 109.5, and 100.5 ppm in the HSQC spectrum, were identified with the help of DQF-COSY and 1D-TOCSY experiments as one rhamnose, one apiose, and one glucose, respectively. Assignments of the NMR chemical shifts of compound **1** were accomplished by 1D-TOCSY, DQF-COSY, HSQC, and HMBC experiments. Key correlation peaks were observed in the HMBC experiment between δ 5.60 (H-1$_{glc}$) and 134.0 (C-3), δ 3.72 (H-2$_{glc}$) and 109.5 (C-1$_{api}$), δ 4.50 (H-1$_{rha}$) and 68.3 (C-6$_{glc}$), δ 4.45 (H-5b$_{api}$) and 4.66 (H-5a$_{api}$) and 168.0 (COO), allowing the substitution sites to be established

between the sugars and the aglycone and the benzoyl group to be located at C-5 of the apiose moiety. The assignment of the sugar configuration was achieved through hydrolysis of **1** with 1 N HCl followed by GC analysis through a chiral column of the obtained monosaccharides treated with 1-(trimethylsilyl)imidazole in pyridine. In the light of these data, the structure of **1** was elucidated as quercetin 3-*O*-(5-*O*-benzoyl)-β-D-apiofuranosyl-(1→2)-*O*-[α-L-rhamnopyranosyl-(1→6)]-β-D-glucopyranoside.

The molecular formula of compound **2** ($C_{43}H_{48}O_{24}$) was determined by its HRESIMS ($[M + Na]^+$ ion at *m/z* 971.2427) and from its ^{13}C NMR data. The negative-ion ESIMS showed a major peak at *m/z* 947 $[M – H]^-$ and several fragments at *m/z* 741 $[M – H – 206]^-$, 609 $[M – H – 206 – 132]^-$, and 301 $[M – H – 206 – 132 – 146 – 162]^-$, indicating the presence of a sinapoyl group and three sugar residues. Comparison of the NMR spectroscopic data of **2** with those of **1** (Table 1) showed that these compounds differed in the acyl moiety linked at C-5 of the apiose, which was identified as a sinapoyl ester moiety in **2** in place of a benzoyl residue in **1**.[15] Hence, compound **2** was elucidated as quercetin 3-*O*-(5-*O*-sinapoyl)-β-D-apiofuranosyl-(1→2)-*O*-[α-L-rhamnopyranosyl-(1→6)]-β-D-glucopyranoside.

The HRESIMS of compound **3** in the positive ion mode showed a $[M + Na]^+$ sodiated molecular ion peak at *m/z* 941.2366, corresponding to a molecular formula of $C_{42}H_{46}O_{23}$. Its ESIMS data showed quasimolecular ion peaks at *m/z* 917 $[M – H]^-$ and 941 $[M + Na]^+$. Three main fragments at *m/z* 741 $[M – H – 176]^-$, 609 $[M – H – 176 – 132]^-$, and 301 $[M – H – 176 – 132 – 146 – 162]^-$, due to the subsequent loss of one feruloyl, one pentose, one deoxyhexose, and one hexose moiety, were also observed. The signals in the ^1H and ^{13}C NMR spectra (Table 1) of **3** were superimposable on those of **1** except for an acyl moiety identified as a feruloyl group ($\delta_{H\alpha}$ 6.13/$\delta_{C\alpha}$ 114.4; δ_{H-5} 6.79/δ_{C-5} 115.8; δ_{H-6} 6.83/δ_{C-6} 123.9; δ_{H-2} 6.96/δ_{C-2} 110.5; $\delta_{H\beta}$ 7.30/$\delta_{C\beta}$ 146.0; δ_{H-OMe} 3.87/δ_{C-OMe} 55.9).[16] From these results, the structure of compound **3** was determined as quercetin 3-*O*-(5-*O*-feruloyl)-β-D-apiofuranosyl-(1→2)-*O*-[α-L-rhamnopyranosyl-(1→6)]-β-D-glucopyranoside.

Compound **4** was obtained as a yellow amorphous powder with the molecular formula, $C_{41}H_{44}O_{22}$, as deduced from the $[M + Na]^+$ peak at *m/z* 911.2236 by HRESIMS and confirmed by ^{13}C NMR data. The ESIMS of compound **4** showed a prominent fragment at *m/z* 887 $[M − H]^-$ and a fragmentation pattern similar to that of the previous compounds **1-3**. The spectroscopic data (Table 1) of the aglycone and sugar moieties were identical to those of **1**, while the acyl moiety differed and was characterized as a *p*-coumaroyl group.[17] Thus, compound **4** was defined as quercetin 3-*O*-(5-*O*-*p*-coumaroyl)-β-D-apiofuranosyl-(1→2)-*O*-[α-L-rhamnopyranosyl-(1→6)]-β-D-glucopyranoside.

Compound **5** was assigned a molecular formula of $C_{27}H_{38}O_{18}$, as deduced from the $[M + Na]^+$ ion at *m/z* 673.1943 in the positive HRESIMS, as well as from analysis of its ^{13}C NMR spectroscopic data (Table 2). The negative ESIMS/MS showed two peaks at *m/z* 607 ($[M −H − 42]^-$) and 527 ($[M − H − 122]^-$) due to the presence of an acetyl and a benzoyl group, respectively. The UV spectrum exhibited an absorption maximum at 280 nm for an aromatic ring conjugated with a carbonyl functionality. The ^1H NMR spectroscopic data (Table 2) showed two anomeric protons at δ 4.54 (d, *J* = 7.8 Hz) and 5.48 (d, *J* = 3.0 Hz), which correlated in the HSQC spectrum with signals at 104.7 and 93.2 ppm; these sugars were characterized as a β-glucose and an α-glucose, respectively. An additional acetal carbon at 105.5 ppm was evident in the ^{13}C NMR spectrum, leading the presence of a fructose moiety to be proposed.[18] 1D-TOCSY, DQF-COSY, and HSQC experiments indicated that compound **5** contains one D-fructose, two D-glucoses, one benzoyl, and one acetyl moiety. The HMBC spectrum indicated the substitution pattern on the molecule of the glycosyl and acyl moieties, showing correlations between δ 4.65 (H-6$_{fru}$) and 168.0 (COO), 5.48 (H-1$_{glc1}$) and 105.5 (C-2$_{fru}$), 4.14 (H-6b$_{glc1}$) and 4.51 (H-6a$_{glc1}$) and 171.0 (COCH$_3$), 4.54 (H-1$_{glc2}$) and 85.5 (C-3$_{glc1}$). Hydrolysis of **5** with 1 N HCl yielded D-glucose and D-fructose as determined by the GC of their trimethylsilylated derivatives on a chiral column. Thus, compound **5** was determined to be β-D-(6-*O*-benzoyl)-fructofuranosyl-(2→1)-[β-D-glucopyranosyl-(1→3)]-6-acetyl-α-D-glucopyranoside.

The molecular formula, $C_{25}H_{36}O_{17}$, was assigned to compound **6** as determined by HRESIMS ([M + Na]$^+$ at *m/z* 631.1848). In the negative ESIMS/MS, fragments at *m/z* 485 [M – H – 122]$^-$, 323 [M – H – 122 – 162]$^-$, and 179 [M – H – 122 – 162 – 162]$^-$ were observed, due to the subsequent loss of a benzoyl and two hexose residues. The UV spectrum was similar to that of **5**, suggesting an oligosaccharide ester structure.[19] Analysis of the NMR data (Table 2) of compound **6** and comparison with those of **5** revealed **6** to differ from **5** only by the absence of the acetyl moiety linked at C-6 of the α-glucose. Thus compound **6** was determined as β-D-(6-*O*-benzoyl)-fructofuranosyl-(2→1)-[β-D-glucopyranosyl-(1→3)]-α-D-glucopyranoside.

The HRESIMS of compound **7** showed a sodiated molecular ion peak at *m/z* 543.2402 [M + Na]$^+$, consistent with a molecular formula of $C_{24}H_{40}O_{12}$. The analysis of the ^{13}C NMR spectrum (Table 2) allowed 13 signals to be attributed to an α-ionol aglycone and 11 to a sugar residue consisting of one hexose and one pentose.[20] The ^{1}H NMR spectrum (Table 2) showed the presence of four methyl groups (δ_H 0.98, 1.15, 1.20, 1.29), two olefinic protons (δ_H 5.74 and 5.97), and one carbinol proton (δ_H 3.75). The DQF-COSY spectrum of **7** indicated for the aglycone, two spin system corresponding to –CH$_2$CHOHCH$_2$– and –CH$_3$CHOHCH=CH– moieties, respectively. A HSQC experiment was used to establish the association of the protons with the corresponding carbons and the HMBC spectrum led to the location of an epoxy group at C-5 and C-6. Additionally, two anomeric proton resonances appeared at δ 4.34 (1H, d, *J* = 7.8 Hz, H-1$_{glc}$) and 4.98 (1H, d, *J* = 3.0 Hz, H-1$_{api}$), which were consistent, when supported by of the ^{13}C NMR spectrum, with a β C-1 configuration for the glucose unit and a β C-1 configuration for the apiose moiety. The absolute configurations of the sugar units were determined as reported for **1**. Definitive evidence of the substitution sites was derived by the HMBC spectrum, which clearly showed cross peaks between δ 1.63 (H-4b) and 2.27 (H-4a) and 64.5 (C-3) and 68.6 (C-5), δ 1.20 (Me-13) and 68.6 (C-5) and 71.3 (C-6), δ 4.40 (H-9) and 102.3 (C-1$_{glc}$), δ 5.97 (H-7) and 71.3 (C-6) and 77.0 (C-9), and δ 4.98 (H-1$_{api}$) and 68.0 (C-6$_{glc}$). The relative configuration at C-3 was assigned as β by comparison with

reported data for similar compounds.[20] From all of these data, **7** was characterized as 3β-hydroxy-5,6-epoxy-β-ionol 9-*O*-β-D-apiofuranosyl-(1→6)-β-D-glucopyranoside.

Compound **8** was assigned a molecular formula of $C_{55}H_{86}O_{24}$, as determined by its positive HRESIMS data (*m/z* 1153.5412 [M + Na]$^+$). The negative ESIMS/MS showed peaks at *m/z* 907 [M − H − 60 − 162]$^-$, 761 [M − H − 60 − 162 − 146]$^-$, 629 [M − H − 60 − 162− 146 − 132]$^-$, due to the presence of an acetyl group, a hexose, a deoxyhexose, and a pentose moiety, respectively. Data from the ^{13}C NMR spectrum (Experimental Section) suggested a triterpenoid bidesmosidic glycoside. The ^{1}H NMR spectrum (Experimental Section) of **8** showed signals for six methyl singlets (δ 0.83, 0.93, 0.96, 1.17, 1.27, and 1.36), two doublet methyl groups at δ 1.08 (*J* = 6.0 Hz) and 1.24 (*J* = 6.5 Hz), two hydroxymethines typical of H-2$_{ax}$ and H-3$_{ax}$ at δ 4.32 (br dd, *J* = 7.5, 4.0 Hz) and 4.11 (d, *J* = 3.0 Hz), a resonance for an olefinic proton at δ 5.32 (t, *J* = 3.5 Hz), four anomeric protons [δ 4.44 d (*J* = 7.8 Hz), 5.10 d (*J* = 1.8 Hz), 5.14 d (*J* = 3.0 Hz), 5.47 d (*J* = 8.0 Hz)], and one acetyl group (δ 2.16, s). The ^{13}C NMR spectrum revealed, for the aglycone moiety, 30 signals that were correlated to the corresponding proton chemical shifts from the HSQC experiment, leading to the identification of the aglycone as 2β,3β-dihydroxyolean-12-en-23,28-dioic acid (medicagenic acid).[21] The structures of the oligosaccharide moieties were deduced using 1D TOCSY, DQF-COSY, HSQC, and HMBC experiments indicating the presence of an inner β-fucopyranose acetylated at the C-4 position (δ$_H$ 5.30, δ$_C$ 73.8), a terminal β-glucopyranose, a terminal α-rhamnopyranose, and a terminal β-apiofuranose (Table 3). The chemical shifts of H-1$_{fuc}$ (δ 5.47) and C-1$_{fuc}$ (94.5 ppm) indicated this sugar moiety to be involved in an ester linkage with the C-28 carboxylic acid group (177.0 ppm) and the HMBC correlation peak between H-1$_{fuc}$-C-28 confirmed this substitution. The configuration of the sugar units was assigned as reported for **1**. The HMBC correlations between H-1$_{glc}$-C-3, H-1$_{rha}$-C-2$_{fuc}$, and H-1$_{api}$-C-3$_{fuc}$ allowed the identification of the sugar sequence. Therefore, compound **8** was identified as 3-*O*-β-D-glucopyranosyl medicagenic

acid   28-*O*-{α-L-rhamnopyranosyl-(1→2)-[β-D-apiofuranosyl-(1→3)]-[4-*O*-acetyl]}-β-D-fucopyranosyl ester.

Compound **9** was isolated only in a small amount. Its molecular formula was determined to be $C_{67}H_{106}O_{35}$ from the HRESIMS and ^{13}C NMR data. The ESIMS of **9** showed a [M − H]$^-$ ion at *m/z* 1469 and prominent fragments at *m/z* 1439 [M − H − 30]$^-$, 1379 [M − H − 30 − 60]$^-$, 1277 [M − H − 30 − 162]$^-$, 1173 [M − H − 30 − 60 − 44 − 162]$^-$, and 1011 [M − H − 30 − 60 − 44 − 162 − 162]$^-$, due to the subsequent loss of a -CH$_2$OH moiety, an acetyl group, a hexose saccharide, a carboxylic group, and another hexose moiety; a saccharide moiety constituted of two hexoses, two deoxyhexoses, and one pentose at *m/z* 747 [162 + 162 + 146 + 146 +132 − H]$^-$ was also evident. Analysis of the NMR data of compound **9** NMR data (Experimental Section and Table 3) led to the determination of the presence of a bidesmosidic triterpenoid saponin with six sugar units and an acetyl group. Comparison of NMR spectra with those of **8** revealed **9** to differ from **8** both in the aglycone moiety and in the sugar chain at C-28, while the β-glucopyranosyl moiety at C-3 was identical. The aglycone of compound **9** showed a hydroxymethylene instead of a methyl group at C-27, allowing its structure to be established as 2β,3β,27-trihydroxyolean-12-en-23,28-dioic acid (presenegenin).[22] The proton-coupling network within each sugar residue was traced using a combination of 1D TOCSY, DQF-COSY, HSQC, and HMBC experiments. These results established that the sugar chain at C-28 in **9** contains one inner β-fucopyranose acetylated at C-4 position (δ_H 5.41, δ_C 75.0), one inner α-rhamnopyranose, one inner β-xylopyranose, one terminal β-glucopyranose, and one terminal β-galactopyranose. ESIMS/MS fragments and HMBC correlations led to establish the linkage among inner sugar units and were in accordance with that reported before for *Polygala* saponin sugar chains.[23] Thus, the structure of 3-*O*-β-D-glucopyranosyl presenegenin   28-*O*-{β-D-galactopyranosyl-(1→4)-β-D-xylopyranosyl-(1→4)-α-L-rhamnopyranosyl-(1→2)-[β-D-glucopyranosyl-(1→3)]-[4-*O*-acetyl]}-β-D-fucopyranosyl ester was tentatively assigned to compound **9**.

Compound **10** was isolated in a trace amount and was not completely pure; its molecular formula was determined to be $C_{65}H_{104}O_{33}$ from the HRESIMS and ^{13}C NMR data. The ESIMS/MS showed peaks at *m/z* 1249 [M – H – 162]⁻, 1187 [M – H – 162– 18 – 44]⁻, 1025 [M – H – 162 – 18 – 44 – 162]⁻, due to the subsequent loss of one hexose, one water molecule, one carboxylic acid, and one hexose unit; the fragment at *m/z* 747 [162 + 162 + 146 + 146 +132 – H]⁻ was again attributed to the saccharide moiety constituted of two hexoses, two deoxyhexoses, and one pentose unit, leading to the proposal of a structure similar to those of saponins **8** and **9**, as described above. Comparison of the NMR spectroscopic data of **10** (Experimental Section and Table 3) with those of **8** and **9** showed that the aglycone moiety of **10** was completely superimposable with that of **8**, while the sugar moieties were identical to those of **9**, except for the absence of the acetyl group on the β-fucopyranose position 4. Therefore, the structure of 3-*O*-β-D-glucopyranosyl medicagenic acid 28-*O*-{β-D-galactopyranosyl-(1→4)-β-D-xylopyranosyl-(1→4)-α-L-rhamnopyranosyl-(1→2)-[β-D-glucopyranosyl-(1→3)]}-β-D-fucopyranosyl ester could be attributed to compound **10**.

Compounds **11-14** were characterized as 3,6'-di-*O*-sinapoylsucrose (**11**),[24] reiniose F (**12**),[25] quercetin 3-*O*-β-D-apiofuranosyl-(1→2)-*O*-[α-L-rhamnopyranosyl-(1→6)]-β-D-glucopyranoside (**13**),[26] and rutin (**14**).[13]

On the basis of previous reports on phenolic derivatives as inhibitors of *h*LDH5,[12,27] phenolic compounds **1-6**, **11-14**, and saponin **8** were assayed on the *h*LDH5 purified isoform to determine their inhibition potencies (Table 4). Most of the compounds were inactive, with IC$_{50}$ values greater than 500 μM, with the exception of two derivatives: compound **12** showed a certain inhibition activity (IC$_{50}$ value of 190.7 μM) and, most notably, compound **11** exhibited an inhibition potency comparable or even slightly better than the reference inhibitor galloflavin,[28] with an IC$_{50}$ value of 90.4 μM.

In order to analyze the possible binding mode of compound **11** into *h*LDH5, molecular docking studies followed by molecular dynamics (MD) simulations and binding energy evaluations were carried out. As a first step, the compound was docked into the catalytic site of *h*LDH5 (4M49 PDB

code) using GOLD software[29] and the ChemPLP fitness scoring function, as this method has already shown to be good in predicting the binding mode of *h*LDH5 inhibitors.[7,30] One hundred different docking poses were generated and clustered, taking into account as a limit value a root-mean-square deviation (RMSD) of 2.0 Å. Ten clusters were obtained and for each of them, a representative docking pose was chosen and subjected to MD simulation to assess the stability of the ten hypothetical binding modes.[31] The complexes were subjected to a total of 22 ns of MD simulation and the resulting trajectories were analyzed in order to measure the stability of docking poses. As shown in Figure 1, the RMSD analysis of the position of the ten docking poses with respect to the input docking highlighted that only two docking poses, corresponding to the first and second cluster, showed an average RMSD below the value of 2.0 Å, calculated for the heavy atoms of the ligand.

The ten trajectories obtained in this way were further analysed through the Molecular Mechanics and Poisson Bolzmann Surface Area (MM-PBSA) method[32] that has been shown to accurately estimate the ligand-receptor energy interaction.[33,34] In this case the MM-PBSA calculations were used for discriminating among different poses suggested by a docking calculation.[35] This approach averages the contributions of gas phase energies, solvation free energies, and solute entropies calculated for snapshots of the complex molecule as well as the unbound components, extracted from MD trajectories, according to the procedure fully described in the Experimental Section. The MM-PBSA results (Table 5) suggested that the first docking pose was the most favorable, as it showed an interaction energy ΔPBSA = -32.2 kcal/mol, more than 8 kcal/mol higher than all the other binding poses. For these reasons, the pose corresponding to the first cluster has been considered as the most reliable binding mode for this compound.

Figure 2 shows the minimized average structure of *h*LDH5 model complexed with compound **11** in the hypothesized binding mode (Cluster 01) obtained from all the 22 ns of the MD simulation. The sucrose part of the molecule interacts in the region of interaction of the nicotinamide fragment of NADH, whereas the two sinapoyl esters explore completely different regions of the LDH5

binding site (see Figures 2A and 2B). A high number of H-bonds stabilizes the binding disposition of compound **11**: as shown in Figure 2C, the sucrose central fragment forms H-bonds with the oxygen backbone of T95, the nitrogen backbone and the carboxamide side-chain of N138. The synapoyl ester attached to the fructose moiety forms an H-bond with the nitrogen backbone of A30 and a lipophilic interaction with Y247; whereas the synapoyl ester attached to the glucose ring forms H-bonds with the nitrogen backbone of Q100 and the side-chain of R106 and shows lipophilic interactions with L109 and P139.

In conclusion, the isolation and structural characterization of compounds **1-14** from *P. flavescens* ssp. *flavescens* is completely in agreement with secondary metabolites already reported in the genus *Polygala*. Moreover, to our knowledge, this is the first report of naturally occurring oligosaccharides as *h*LDH5 inhibitors, being a new interesting scaffold for the potential development of new anticancer agents.

EXPERIMENTAL SECTION

General Experimental Procedures. An Atago AP-300 digital polarimeter with a sodium lamp (589 nm) and 1 dm microcell was used to measure optical rotations. UV spectra were registered on a Perkin-Elmer Lambda spectrophotometer. NMR experiments were recorded on a Bruker DRX-600 spectrometer equipped with a Bruker 5 mm TCI CryoProbe, acquiring the spectra in methanol-d_4. Standard pulse sequences and phase cycling were used for TOCSY, HSQC, DQF-COSY, and HMBC NMR experiments. NMR data were processed using XWIN-NMR software. HRESIMS were obtained in the positive- and negative-ion mode on a Q-TOF premier spectrometer equipped with a nanospray ion source (Waters Milford, MA, USA). ESIMS were obtained from an LCQ Advantage ThermoFinnigan spectrometer (ThermoFinnigan, USA). Column chromatography was performed over Sephadex LH-20. HPLC analysis was performed using a Shimadzu LC-8A series

pumping system equipped with a Shimadzu RID-10A refractive index detector and Shimadzu injector on a C_{18} μ-Bondapak column (30 cm × 7.8 mm, 10 μm Waters, flow rate 2.0 mL/min). TLC separations were carried out using silica gel 60 F_{254} (0.20 mm thickness) plates (Merck) with *n*-BuOH-CH_3COOH-H_2O (60:15:25) as eluent and cerium sulphate as spray reagent. GC analysis was performed using a Dani GC 1000 instrument on a L-CP-Chirasil-Val column (0.32 mm × 25 m) working with the following temperature program: 100 °C for 1 min, ramp of 5 °C/min up to 180 °C; injector and detector temperature 200 °C; carrier gas N_2 (2 mL/min); detector dual FID; split ratio 1:30; injection 5 μL.

Plant Material. The aerial parts of flowering *Polygala flavescens* ssp. *flavescens* were collected in the Cerbaie hills, Castelfranco di Sotto (Pisa, Italy), 43.751228 N, 10.719234 E, on May 7th, 2015. The plant was identified by the identification keys available in Arrigoni (2014).[36] A voucher specimen (4273_*Polygala_flavescens*_ssp._*flavescens*/5) was deposited at Herbarium Horti Botanici Pisani (PI, acronym following Thiers, 2017).[37]

Extraction and Isolation. The powdered dried aerial parts of *P. flavescens* ssp. *flavescens* (370 g) were defatted with *n*-hexane and then extracted with MeOH (3 × 2 L), to give 71.1 g of dried residue. The MeOH extract was partitioned between AcOEt, *n*-BuOH, and H_2O to give 11.5 g, 15.5 g, and 36.2 g of the respective dried residues, together with 7.0 g of compound **14** obtained as abundant precipitate. Sephadex LH-20 column chromatography (5 × 100 cm) was used to separate the *n*-BuOH soluble fraction (10 g), using MeOH as eluent at a flow rate of 2.0 mL/min, with fractions of 12 mL collected and grouped into fourteen major fractions (A-N). Fraction N gave pure compound **14** (100 mg). Fractions A (424 mg), B (556 mg), and C (242 mg) were separately submitted to HPCPC with $CHCl_3$-MeOH-H_2O-*i*-PrOH (5:6:4:1) in which the stationary phase consisted of the lower phase (ascending mode, flow rate 3 mL/min), with fractions of 3 mL collected. HPCPC fractions A_2 (50 mg) and B_2 (46 mg) were chromatographed by RP-HPLC with MeOH-H_2O (5.5:4.5) to afford compound **9** (1.0 mg, t_R 13 min), from fraction A_2 and compound **10** (0.5 mg, t_R 17 min) from fraction B_2. HPCPC fraction C_8 (35 mg) after separation with RP-HPLC

with MeOH-H_2O (3:2) yielded compound **8** (4.2 mg, t_R 24 min). Fraction E (196.5 mg) was purified by RP-HPLC with MeOH-H_2O (2.5:7.5) as eluent to yield compound **7** (1.6 mg, t_R 19 min). Fraction F (524 mg) was subjected to RP-HPLC with MeOH-H_2O (3:7) to yield compounds **6** (3.8 mg, t_R 17 min) and **5** (7.2 mg, t_R 50 min). Fractions H (1948 mg), I (584.6 mg), and J (774 mg) were chromatographed over RP-HPLC with MeOH-H_2O (2:3) to obtain compound **12** (4.4 mg, t_R 39 min), from fraction H, compounds **13** (3.4 mg, t_R 21 min), **11** (5.0 mg, t_R 27 min), and **1** (6.1 mg, t_R 72 min), from fraction I, compounds **13** (14 mg, t_R 16 min) and **2** (4.4 mg, t_R 24 min), from fraction J. Fraction K (217 mg) was purified by RP-HPLC with MeOH-H_2O (5.5:4.5) to yield compounds **13** (11.7 mg, t_R 14 min), **14** (16 mg, t_R 19 min), and **3** (8 mg, t_R 26 min). Fraction M (453 mg) was subjected to RP-HPLC with MeOH-H_2O (4.5:5.5) to yield compounds **14** (5.4 mg, t_R 13 min), **3** (3.1 mg, t_R 16 min), and **4** (15.0 mg, t_R 17 min).

Compound (1): yellow amorphous powder; $[\alpha]_D^{25}$ -42 (*c* 0.1, MeOH); UV (MeOH) λ_{max} (log ε) 260 (4.00), 356 (3.92) nm; ^{1}H and ^{13}C NMR, see Table 1; ESIMS *m/z* 845 [M − H]$^-$, 723 [M − H − 122]$^-$, 591 [M − H − 122 − 132]$^-$, 869 [M + Na]$^+$, 723 [M + Na − 146]$^+$; HRESIMS *m/z* 869.2102 [M + Na]$^+$, 847.2297 [M + H]$^+$ (calcd for $C_{39}H_{42}O_{21}Na$ 869.2116, $C_{39}H_{43}O_{21}$ 847.2297).

Compound (2): yellow amorphous powder; $[\alpha]_D^{25}$ -25 (*c* 0.1, MeOH); UV (MeOH) λ_{max} (log ε) 240 sh (3.76), 268 sh (3.90), 335 (3.85) nm; ^{1}H and ^{13}C NMR, see Table 1; ESIMS *m/z* 947 [M − H]$^-$, 741 [M − H − 206]$^-$, 609 [M − H − 206 − 132]$^-$, 301 [M − H − 206 − 132 − 146 − 162]$^-$; HRESIMS *m/z* 971.2427 [M + Na]$^+$, 949.2626 [M + H]$^+$ (calcd for $C_{43}H_{48}O_{24}Na$ 971.2433, $C_{43}H_{49}O_{24}$ 949.2614).

Compound (3): yellow amorphous powder; $[\alpha]_D^{25}$ -62 (*c* 0.1, MeOH); UV (MeOH) λ_{max} (log ε) 250 sh (3.75), 270 sh (3.93), 259 sh (3.78), 334 (3.91) nm; ^{1}H and ^{13}C NMR, see Table 1; ESIMS *m/z* 917 [M − H]$^-$, 741 [M − H − 176]$^-$, 609 [M − H − 176 − 132]$^-$, 301 [M − H − 176 − 132 − 146 − 162]$^-$, 941 [M + Na]$^+$, 795 [M + Na − 146]$^+$; HRESIMS *m/z* 941.2366 [M + Na]$^+$, 919.2547 [M + H]$^+$ (calcd for $C_{42}H_{46}O_{23}Na$ 941.2328, $C_{42}H_{47}O_{23}$ 919.2508).

Compound (4): yellow amorphous powder; $[\alpha]_D^{25}$ -104 (*c* 0.1, MeOH); UV (MeOH) λ_{max} (log ε) 258 sh (3.93), 269 (4.05), 320 (3.88) nm; ^{1}H and ^{13}C NMR, see Table 1; ESIMS *m/z* 887 [M − H]$^-$, 741 [M − H − 146]$^-$, 609 [M − H − 146 − 132]$^-$, 301 [M − H − 146 − 132 − 146 − 162]$^-$, 911 [M + Na]$^+$, 765 [M + Na − 146]$^+$; HRESIMS *m/z* 911.2236 [M + Na]$^+$, 889.2420 [M + H]$^+$ (calcd for $C_{41}H_{44}O_{22}Na$ 911.2222, $C_{41}H_{45}O_{22}$ 889.2402).

Compound (5): pale yellow amorphous powder; $[\alpha]_D^{25}$ +23 (*c* 0.1, MeOH); UV (MeOH) λ_{max} (log ε) 228 (3.78), 280 (3.92) nm; ^{1}H and ^{13}C NMR, see Table 2; ESIMS *m/z* 649 [M − H]$^-$, 607 [M − H − 42]$^-$, 589 [M − H − 60]$^-$, 527 [M − H − 122]$^-$, 673 [M + Na]$^+$, 407 [M + Na − 266]$^+$; HRESIMS *m/z* 673.1943 [M + Na]$^+$ (calcd for $C_{27}H_{38}O_{18}Na$ 673.1956).

Compound (6): pale yellow amorphous powder; $[\alpha]_D^{25}$ +20 (*c* 0.1, MeOH); UV (MeOH) λ_{max} (log ε) 225 (3.77), 282 (3.90) nm; ^{1}H and ^{13}C NMR, see Table 2; ESIMS *m/z* 607 [M − H]$^-$, 485 [M − H − 122]$^-$, 323 [M − H − 122 − 162]$^-$, 179 [M − H −122 − 162 − 162]$^-$, 631 [M + Na]$^+$, 469 [M + Na − 162]$^+$, 347 [M + Na − 162 − 122]$^+$, 185 [M + Na − 162 − 122 − 162]$^+$; HRESIMS *m/z* 631.1848 [M + Na]$^+$ (calcd for $C_{25}H_{36}O_{17}Na$ 631.1850).

Compound (7): amorphous powder; $[\alpha]_D^{25}$ +14 (*c* 0.1, MeOH); ^{1}H and ^{13}C NMR, see Table 2; ESIMS *m/z* 543 [M + Na]$^+$, 1063 [2M + Na]$^+$; HRESIMS *m/z* 543.2402 [M + Na]$^+$ (calcd for $C_{24}H_{40}O_{12}Na$ 543.2417).

Compound (8): amorphous powder; $[\alpha]_D^{25}$ +36 (*c* 0.1, MeOH); ^{1}H NMR data of the aglycone (CD$_3$OD, 600 MHz) δ 0.83 (3H, s, Me-26), 0.93 (3H, s, Me-29), 0.96 (1H, overlapped, H-16b), 0.96 (3H, s, Me-30), 1.16 (1H, m, H-19b), 1.17 (3H, s, Me-27), 1.21 (1H, overlapped, H-15b), 1.22 (1H, overlapped, H-21b), 1.24 (1H, overlapped, H-1b), 1.27 (3H, s, Me-25), 1.28 (1H, overlapped, H-6b), 1.35 (1H, overlapped, H-7b), 1.36 (3H, s, Me-24), 1.41 (1H, m, H-21a), 1.54 (1H, overlapped, H-7a), 1.55 (1H, overlapped, H-22b), 1.59 (1H, m, H-6a), 1.60 (1H, overlapped, H-9), 1.62 (1H, overlapped, H-11b), 1.63 (2H, overlapped, H-5 and H-16a), 1.68 (1H, m, H-15a), 1.74 (1H, m, H-19a), 1.85 (1H, ddd, *J* = 16.0, 13.5, 4.0 Hz, H-22a), 2.08 (1H, m, overlapped, H-11a), 2.10, (1H,

overlapped, H-1a), 2.87 (1H, dd, J = 13.5, 3.0 Hz, H-18), 4.11 (1H, d, J = 3.0 Hz, H-3), 4.32 (1H, br dd, J = 7.5, 4.0 Hz, H-2), 5.32 (1H, t, J = 3.5 Hz, H-12); ^{13}C NMR data of the aglycone (CD$_3$OD, 150 MHz) δ 13.4 (C-24), 16.4 (C-25), 17.0 (C-26), 20.8 (C-6), 23.5 (C-16 and C-30), 23.6 (C-11), 25.6 (C-27), 28.3 (C-15), 31.2 (C-22), 31.3 (C-20), 32.8 (C-29), 33.0 (C-7), 34.4 (C-21), 36.7 (C-10), 41.0 (C-8), 42.0 (C-18), 42.7 (C-14), 44.1 (C-1), 46.0 (C-19), 47.4 (C-17), 48.8 (C-9), 52.5 (C-5), 52.8 (C-4), 70.8 (C-2), 86.0 (C-3), 122.4 (C-12), 144.0 (C-13), 177.0 (C-28), 185.0 (C-23); ^{1}H and ^{13}C NMR of the sugar moieties, see Table 3; ESIMS m/z 1129 [M − H]$^-$, 907 [M − H − 60 − 162]$^-$, 761 [M − H − 60 − 162 − 146]$^-$, 629 [M − H − 60 − 162− 146 − 132]$^-$, 1153 [M + Na]$^+$; HRESIMS m/z 1153.5412 [M + Na]$^+$ (calcd for C$_{55}$H$_{86}$O$_{24}$Na 1153.5328).

Compound (9): amorphous powder; $[\alpha]_D^{25}$-112 (*c* 0.1, MeOH); ^{1}H NMR data of the aglycone (CD$_3$OD, 600 MHz) δ 0.75 (3H, s, Me-26), 0.92 (3H, s, Me-30), 0.93 (3H, s, Me-29), 1.21 (1H, m, H-19b), 1.25 (1H, overlapped, H-21b), 1.27 (3H, s, Me-25), 1.29 (1H, overlapped, H-7b), 1.32 (1H, overlapped, H-16b), 1.30 (1H, overlapped, H-6b), 1.36 (3H, s, Me-24), 1.37 (1H, m, H-21a), 1.59 (1H, overlapped, H-7a), 1.60 (2H, overlapped, H-6a and H-22b), 1.61 (1H, overlapped, H-19a), 1.64 (2H, overlapped, H-11b and H-16a), 1.65 (2H, overlapped, H$_2$-15), 1.70 (1H, overlapped, H-5), 1.88 (1H, overlapped, H-9), 2.00 (1H, m, overlapped, H-11a), 2.08 (1H, dd, J = 13.0, 3.0 Hz, H-1b), 2.28 (1H, overlapped, H-1a), 2.37 (1H, m, H-22a), 2.80 (1H, dd, J = 13.5, 3.0 Hz, H-18), 3.76 (1H, overlapped, H-27b), 3.79 (1H, overlapped, H-27a), 4.09 (1H, d, J = 2.5 Hz, H-3), 4.29 (1H, br dd, J = 7.0, 3.5 Hz, H-2), 5.66 (1H, t, J = 3.5 Hz, H-12); ^{13}C NMR data of the aglycone (CD$_3$OD, 150 MHz) δ 14.0 (C-24), 16.5 (C-25), 18.0 (C-26), 21.5 (C-6), 23.0 (C-30), 23.7 (C-11 and C-16), 25.0 (C-15), 31.0 (C-20), 32.0 (C-7), 33.0 (C-29), 34.3 (C-21), 34.7 (C-22), 37.1 (C-10), 41.0 (C-8), 42.0 (C-18), 44.4 (C-18), 44.7 (C-1), 46.2 (C-19), 47.4 (C-17), 48.3 (C-14), 49.0 (C-9), 52.0 (C-5), 52.5 (C-4), 62.3 (C-27), 71.2 (C-2), 83.1 (C-3), 128.4 (C-12), 139.2 (C-13), 177.0 (C-28), 180.0 (C-23); ^{1}H and ^{13}C NMR of the sugar moieties, see Table 3; ESIMS m/z 1469 [M − H]$^-$, 1439 [M − H − 30]$^-$, 1379 [M − H − 30 − 60]$^-$, 1277 [M − H − 30 − 162]$^-$, 1215 [M − H − 162− 18 − 44]$^-$, 1173 [M − H − 30 − 60 − 44 − 162]$^-$, 1155 [M − H − 30 − 60 − 18 − 44 − 162]$^-$, 1011 [M − H − 30 − 60 − 44 − 162 −

16

162]⁻, 907 [M – H – 30 – 18 – 44 – 162 – 162 –146]⁻, 747 [162 + 162 + 146 + 146 +132 – H]⁻, 438 [747 – 162 – 146 – H]⁻; HRESIMS *m/z* 1493.6470 [M + Na]⁺ (calcd for $C_{67}H_{106}O_{35}Na$ 1493.6412).

Compound (10): amorphous powder; $[\alpha]_D^{25}$-135 (*c* 0.1, MeOH); ¹H and ¹³C NMR data of the aglycone moiety were superimposable on those reported for **8**; ¹H and ¹³C NMR of the sugar moieties, see Table 3; ESIMS *m/z* 1411 [M – H]⁻, 1249 [M – H – 162]⁻, 1187 [M – H – 162– 18 – 44]⁻, 1025 [M – H – 162 – 18 – 44 – 162]⁻, 1007 [M – H – 162 – 18 – 44 – 162 – 18]⁻, 747 [162 + 162 + 146 + 146 +132 – H]⁻, 585 [747 – 162 – H]⁻, 439 [747 – 162 – 146 – H]⁻; HRESIMS *m/z* 1493.6470 [M + Na]⁺ (calcd for $C_{67}H_{106}O_{35}Na$ 1493.6412).

Acid Hydrolysis of Compounds 1-10. Acid hydrolysis of compounds **1-10** was carried out as reported in a previous report.[38] D-Glucose, D-apiose, D-xylose, L-rhamnose, D-galactose, and D-fucose were identified as the sugar moiety in each case by comparison with the retention times of authentic samples.

LDH Assays. Isolated compounds were evaluated against purified human lactate dehydrogenase isoform 5 (Lee Biosolution, Inc.). The enzymatic reaction was performed in the ''forward'' direction (pyruvate to lactate) and the amount of consumed NADH was monitored (emission wavelength at 460 nm, excitation wavelength at 340 nm). Assays were carried out in 96-well plates, by using 100 mM phosphate buffer (pH = 7.4), in the presence of 200 μM pyruvate and 40 μM NADH. Compounds were dissolved in DMSO stock solutions at the maximum concentration of 500 μM (the concentration of DMSO did not exceed 4% during the measurements) and seven different concentrations (from 500 to 0.7 μM, in duplicate for each concentration) for each compound were used to generate the concentration-response curve. If background fluorescence or NADH fluorescence quenching (caused by the compounds) was observed, it was subtracted from the measurements. After 15 min of incubation, the final measurements were carried out by using a Victor X3 Microplate Reader (Perkin Elmer). IC_{50} values were produced using GraphPad Prism software (GraphPad, San Diego, CA, USA).

Docking Studies. The crystal structure of *h*LDH5 (4M49 PDB code)[37] was taken from the Protein Data Bank.[40] After adding hydrogen atoms the protein complexed with its reference inhibitor was minimized using AMBER14 software[41] and parm03 force field at 300 K (in order to reproduce the room temperature used in the enzymatic assay). The complex was placed in a rectangular parallelepiped water box, an explicit solvent model for water (TIP3P) was used and the complexes were solvated with a 20 Å water cap. Chlorine ions were added as counterions to neutralize the system. Two steps of minimization were then carried out; in the first stage, the protein was kept fixed with a position restraint of 500 kcal/mol·Å^2 and the positions of the water molecules were solely minimized. In the second stage, the entire system was minimized through 5000 steps of steepest descent followed by conjugate gradient (CG) until a convergence of 0.05 kcal/Å·mol. The ligand was built using Maestro[42] and was minimized by means of Macromodel[43] in a water environment following the CG method until a convergence value of 0.05 kcal/Å·mol, using the MMFFs force field and a distance-dependent dielectric constant of 1.0. Automated docking was carried out by means of the GOLD 5.1 program. The region of interest for the docking studies was defined in such a manner that it contained all residues within 10 Å of the reference ligand and NADH in the X-ray crystal structure (4M49 PDB code). The "allow early termination" command was deactivated, while the possibility for the ligand to flip ring corners was activated. The remaining GOLD default parameters were used, and the ligands were submitted to 100 genetic algorithm runs by applying the ChemPLP fitness function. An RMSD tolerance of 2.0 Å was used to carry out the cluster analysis of the docking solutions, and all the other settings were left as their defaults. The ten clusters of solutions thus obtained were taken into account.

Molecular Dynamic Simulations. The simulations were performed using AMBER14 and the input preparation and minimization stages were the same reported above. Molecular dynamics trajectory was then run using the energy minimized structure as the input, and particle mesh Ewald electrostatics[44] and periodic boundary conditions were used in the simulation. The time step of the simulations was 2.0 fs with a cutoff of 12 Å for the non-bonded interaction. SHAKE was employed

to keep all bonds involving hydrogen atoms rigid. The General Amber Force Field (GAFF) parameters were assigned to the ligand. The partial charges were calculated using the AM1-BCC method, as implemented in the Antechamber suite of AMBER14. The first MD step consisted of 2.0 ns of constant-volume simulation in which the temperature of the system was raised from 0 to 300 K. In the second step a 10 ns constant pressure simulation was carried out to equilibrate the system, and the temperature of the system was kept constant at 300 K by using the Langevin thermostat. In both the first and second step, a harmonic potential of 10 kcal/(mol·Å^2) was applied to the protein α-carbons. Step 3 consisted of a 10 ns simulation that was performed using the conditions used in step 2, but without applying any position restraint in order to leave the system completely free. A total of 22 ns of MD simulation was thus performed for each analyzed ligand-protein complex.

Evaluation of Binding Energy. Evaluation of the binding energy of the ligand-protein complexes analyzed through MD simulations was carried out using AMBER14. The trajectories relative to the last 10 ns of each simulation were extracted and used for the calculation for a total of 100 snapshots (at time intervals of 100 ps). Van der Waals, electrostatic, and internal interactions were calculated with the SANDER module of AMBER14, whereas polar energies were calculated using the Poisson-Boltzman methods with the MM-PBSA module of AMBER14. Dielectric constants of 1 and 80 were used to represent the gas and water phases, respectively, while the MOLSURF program was employed to estimate the nonpolar energies. The entropic term was considered as approximately constant in the comparison of the ligand-protein energetic interactions.

ASSOCIATED CONTENT

Supporting Information. HRESIMS and NMR spectra of compounds **1-10**. This material is available via the Internet at http://pubs.acs.org.

AUTHOR INFORMATION

Corresponding Author

*Tel: +39-089-969754. Fax: +39-089-969602. E-mail: detommasi@unisa.it

Notes

The authors declare no competing financial interest.

References

(1) Eriksen, B.; Persson, C. In *The Families and Genera of Vascular Plants*; Kubitzki, K., Ed.; Springer-Verlag: Berlin, 2007; Vol. 9, pp 345-363.

(2) Klein, L. C. Jr.; Faloni de Andrade, S.; Cechinel Filho, V. *Chem. Biodivers*. **2012**, *9*, 181-209.

(3) Dall'Acqua, S.; Viola, G.; Cappelletti, E. M.; Innocenti, G. *Z. Naturforsch. C* **2004**, *59*, 335-338.

(4) Kobayashi, S.; Miyase, T.; Noguchi, H. *J. Nat. Prod*. **2002**, *65*, 319-328.

(5) Peruzzi, L.; Conti, F.; Bartolucci, F. *Phytotaxa* **2014**, *168*, 1-75.

(6) Peruzzi, L.; Domina, G.; Bartolucci, F.; Galasso, G.; Peccenini, S.; Raimondo, F. M.; Albano, A.; Alessandrini, A.; Banfi, E.; Barberis, G.; Bernardo, L.; Bovio, M.; Brullo, S.; Brundu, G.; Brunu, A.; Camarda, I.; Carta, L.; Conti, F.; Croce, A.; Iamonico, D.; Iberite, M.; Iiriti, G.; Longo, D.; Marsili, S.; Medagli, P.; Pistarino, A.; Salmeri, C.; Santangelo, A.; Scassellati, E.; Selvi, F.; Soldano, A.; Stinca, A.; Villani, M.; Wagensommer, R. P.; Passalacqua, N. G. *Phytotaxa* **2015**, 196, 1-217.

(7) Granchi, C.; Roy, S.; Del Fiandra, C.; Tuccinardi, T.; Lanza, M.; Betti, L.; Giannaccini, G.; Lucacchini, A.; Martinelli, A.; Macchia, M.; Minutolo, F. *MedChemComm* **2011**, *2*, 638-643.

(8) Bader, A.; Tuccinardi, T.; Granchi, C.; Martinelli, A.; Macchia, M.; Minutolo, F.; De Tommasi, N.; Braca, A. *Phytochemistry* **2015**, *116*, 262-268.

(9) Martinez-Outschoorn, U. E.; Peiris-Pagés, M.; Pestell, R. G.; Sotgia, F.; Lisanti, M. P. *Nat. Rev. Clin. Oncol.* **2017**, *14*, 11-31.

(10) Granchi, C.; Paterni, I.; Rani, R.; Minutolo F. *Future Med. Chem*. **2013**, *5*,1967-1991.

(11) Deiab, S.; Mazzio, E.; Messeha, S.; Mack, N.; Soliman, K. F. *Eur. J. Med. Plants* **2013**, *3*, 603-615.

(12) Grabowski, M.; Banecki, B.; Kadziński, L.; Jakóbkiewicz-Banecka, J.; Kaźmierkiewicz, R.; Gabig-Cimińska, M.; Węgrzyn, G.; Węgrzyn, A.; Banecka-Majkutewicz, Z. *Biochem. Biophys. Res. Commun.* **2015**, *465*, 363-367.

(13) Agrawal, P. K. *Carbon-13 NMR of Flavonoids;* Elsevier: Amsterdam, 1989; p 341.

(14) Warnock, M. J.; Liu, Y. L.; Mabry, T. J. *Phytochemistry* **1983**, *22*, 1834-1835.

(15) Fan, Q-L.; Zhu, Y-D.; Huang, W-H.; Qi, Y.; Guo, B-L. *Molecules* **2014**, *19*, 11341-11349.

(16) Kim, Y.; Park, E. J.; Kim, J.; Kim, Y-B.; Kim, S. R.; Kim, Y. C. *J. Nat. Prod.* **2001**, *64*, 75-78.

(17) Vitalini, S.; Braca, A.; Passarella, D.; Fico, G. *Fitoterapia* **2010**, *81*, 940-947.

(18) Kobayashi, S.; Miyase, T.; Noguchi, H. *J. Nat. Prod.* **2002**, *65*, 319-328.

(19) Zhang, D.; Miyase, T.; Kuroyanagi, M.; Umehara, K.; Noguchi, H. *Phytochemistry* **1998**, *47*, 45-52.

(20) Sudo, H.; Ide, T.; Otsuka, H.; Hirata, E.; Takushi, A.; Shinzato, T.; Takeda, Y. *Chem. Pharm. Bull.* **2000**, *48*, 542-546.

(21) Sakai, K.; Nagao, T.; Okabe, H. *Phytochemistry* **1999**, *51*, 309-318.

(22) Zhang, D.; Miyase, T.; Kuroyanagi, M.; Umehara, K.; Ueno, A. *Chem. Pharm. Bull.* **1996**, *44*, 173-179.

(23) Yoshikawa, M.; Murakami, T.; Matsuda, H.; Takahiro, U.; Kadoya, M.; Yamahara, J.; Murakami, N. *Chem. Pharm. Bull.* **1996**, *44*, 1305-1313.

(24) Ikeya, Y.; Sugama, K.; Okada, M.; Mitsuhashi, H. *Chem. Pharm. Bull.* **1991**, *39*, 2600-2605.

(25) Saitoh, H.; Miyase, T.; Ueno, A. *Chem. Pharm. Bull.* **1994**, *42*, 1879-1885.

(26) Rastrelli, L.; Saturnino, P.; Schettino, O.; Dini, A. *J. Agric. Food. Chem.* **1995**, *43*, 2020-2024.

(27) Deiab, S.; Mazzio, E.; Eyunni, S.; McTier, O.; Mateeva, N.; Elshami, F.; Soliman, K. F. *Evid. Based Complement. Alternat. Med.* **2015**, *2015*, 276946.

(28) Manerba, M.; Vettraino, M.; Fiume, L.; Di Stefano, G.; Sartini, A.; Giacomini, E.; Buonfiglio, R.; Roberti, M.; Recanatini, M. *ChemMedChem* **2012**, *7*, 311-317.

(29) Verdonk, M. L.; Cole, J. C.; Hartshorn, M. J.; Murray, C. W.; Taylor, R. D. *Proteins* **2003**, *52*, 609-623.

(30) Calvaresi, E. C.; Granchi, C.; Tuccinardi, T.; Di Bussolo, V.; Huigens, R. W., 3rd; Lee, H. Y.; Palchaudhuri, R.; Macchia, M.; Martinelli, A.; Minutolo, F.; Hergenrother, P. J. *ChemBioChem* **2013**, *14*, 2263-2267.

(31) Mocan, A.; Zengin, G.; Simirgiotis, M.; Schafberg, M.; Mollica, A.; Vodnar, D. C.; Crişan, G.; Rohn, S. *J. Enz. Inhib. Med. Chem.* **2017**, *32*, 153-168.

(32) Kollman, P. A.; Massova, I.; Reyes, C.; Kuhn, B.; Huo, S.; Chong, L.; Lee, M.; Lee, T.; Duan, Y.; Wang, W.; Donini, O.; Cieplak, P.; Srinivasan, J.; Case, D. A.; Cheatham, T. E., 3rd. *Acc. Chem. Res.* **2000**, *33*, 889-897.

(33) Tuccinardi, T.; Manetti, F.; Schenone, S.; Martinelli, A.; Botta, M. *J. Chem. Inf. Model* **2007**, *47*, 644-655.

(34) Tuccinardi, T.; Granchi, C.; Iegre, J.; Paterni, I.; Bertini, S.; Macchia, M.; Martinelli, A.; Qian, Y.; Chen, X.; Minutolo, F. *Bioorg. Med. Chem. Lett.* **2013**, *23*, 6923-6927.

(35) Petrou, A.; Geronikaki, A.; Terzi, E.; Guler, O. O.; Tuccinardi, T.; Supuran, C. T. *J. Enz. Inhib. Med. Chem.* **2016**, *31*, 1306-1311.

(36) Arrigoni, P.V. *Inform. Bot. Ital*. **2014**, *46*, 235-263.

(37) Thiers, B. *Index Herbariorum: A Global Directory of Public Herbaria and Associated Staff*, 2017. http://sweetgum.nybg.org/ih/.

(38) Milella, L.; Milazzo, S.; De Leo, M.; Vera Saltos, M. B.; Immacolata, F.; Tuccinardi, T.; Lapillo, M.; De Tommasi, N.; Braca, A. *J. Nat. Prod.* **2016**, *79*, 2104-2112.

(39) Fauber, B. P.; Dragovich, P. S.; Chen, J.; Corson, L. B.; Ding, C. Z.; Eigenbrot, C.; Giannetti, A. M.; Hunsaker, T.; Labadie, S.; Liu, Y.; Malek, S.; Peterson, D.; Pitts, K.; Sideris, S.; Ultsch, M.;

VanderPorten, E.; Wang, J.; Wei, B.; Yen, I.; Yue, Q. *Bioorg. Med. Chem. Lett.* **2013**, *23*, 5533-5539.

(40) Berman, H. M.; Westbrook, J.; Feng, Z.; Gilliland, G.; Bhat, T. N.; Weissig, H.; Shindyalov, I. N.; Bourne, P. E. *Nucleic Acids Res.* **2000**, *28*, 235-242.

(41) Case, D. A.; Berryman, J. T.; Betz, R. M.; Cerutti, D. S.; III, T. E. C.; Darden, T. A.; Duke, R. E.; Giese, T. J.; Gohlke, H.; Goetz, A. W.; Homeyer, N.; Izadi, S.; Janowski, P.; Kaus, J.; Kovalenko, A.; Lee, T. S.; LeGrand, S.; Li, P.; Luchko, T.; Luo, R.; Madej, B.; Merz, K. M.; Monard, G.; Needham, P.; Nguyen, H.; Nguyen, H. T.; Omelyan, I.; Onufriev, A.; Roe, D. R.; Roitberg, A.; Salomon-Ferrer, R.; Simmerling, C. L.; Smith, W.; Swails, J.; Walker, R. C.; Wang, J.; Wolf, R. M.; Wu, X.; York, D. M.; Kollman, P. A. *AMBER*, version 14; University of California: San Francisco, CA, 2015.

(42) *Maestro*, version 9.0; Schrödinger, Inc.: Portland, OR, 2009.

(43) *Macromodel*, version 9.7; Schrödinger, Inc.: Portland, OR, 2009.

(44) Essmann, U.; Perera, L.; Berkowitz, M. L.; Darden, T.; Lee, H.; Pedersen, L. G. *J. Chem. Phys.* **1995**, *103*, 8577-8593.

1 R =

2 R =

3 R =

4 R =
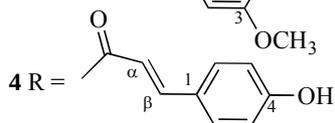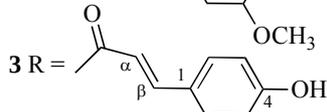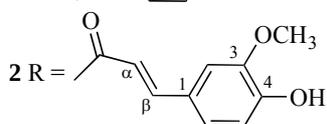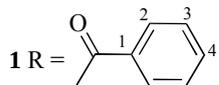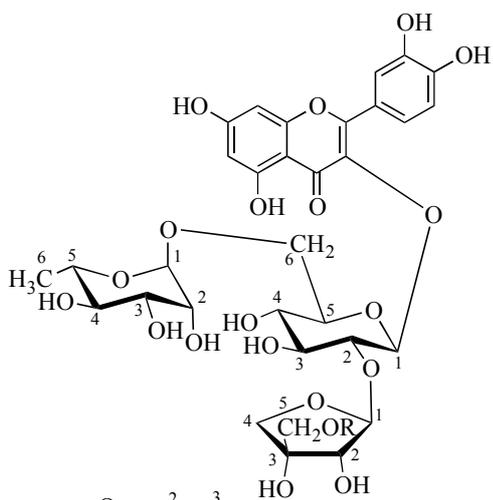
13 R = H
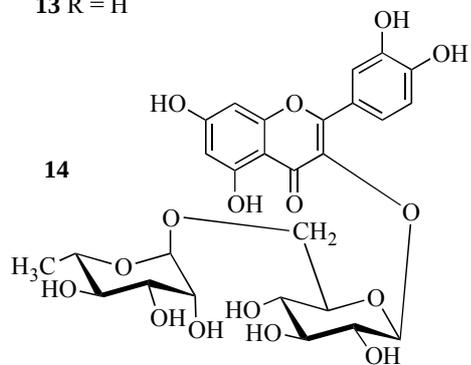
14
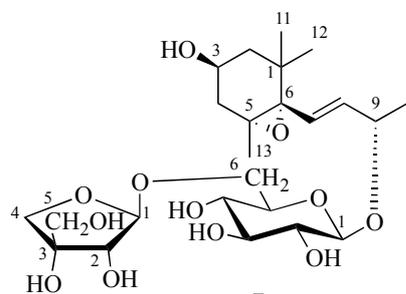
7
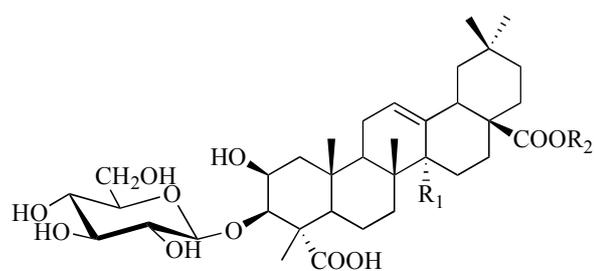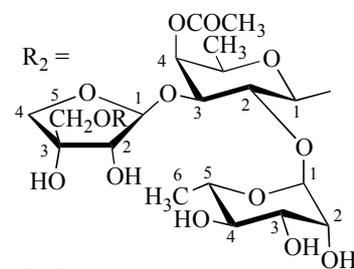
8 R₁ = CH₃   R₂ =

9 R₁ = CH₂OH   R₂ =
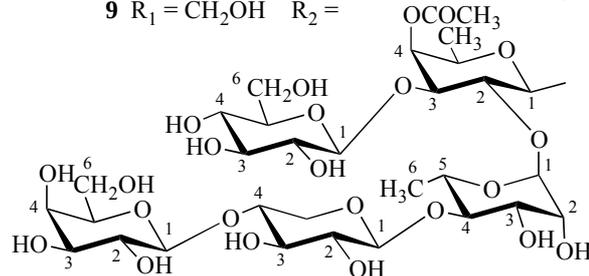
10 R₁ = CH₃   R₂ =
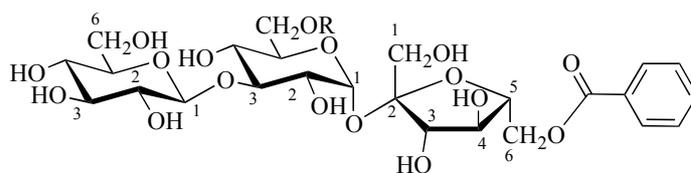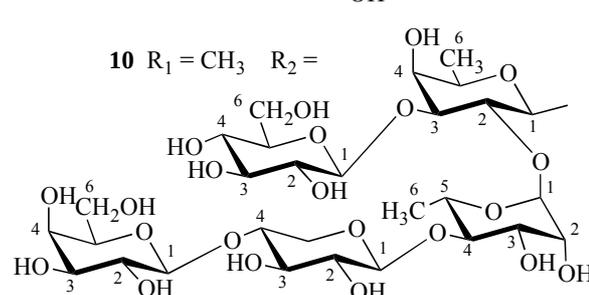
5 R = COCH₃

6 R = H

11 R = H

12 R = CH₂OH
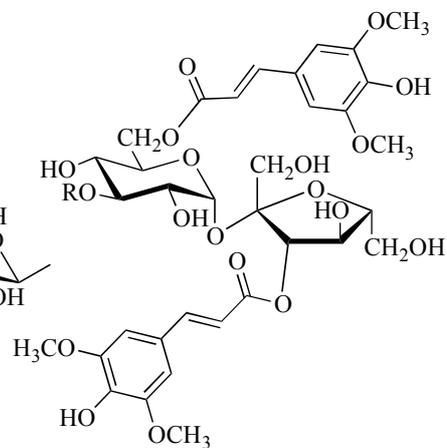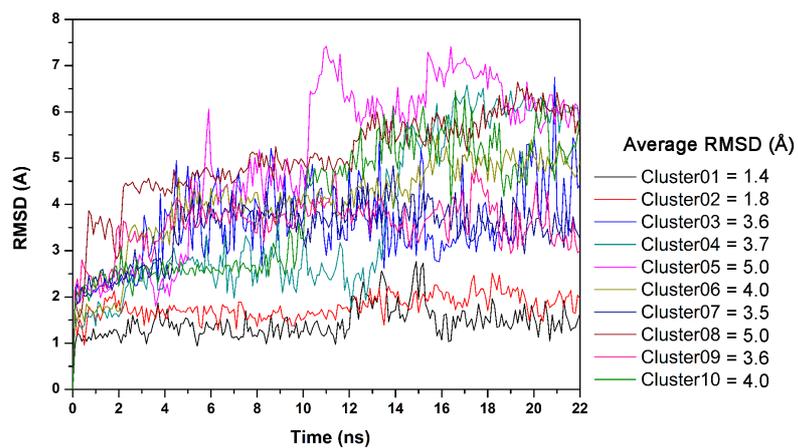
Figure 1. Analysis of the MD simulations. The plot shows the RMSD (Å) of the position of the heavy atoms of the ten docking poses of compound **11**.
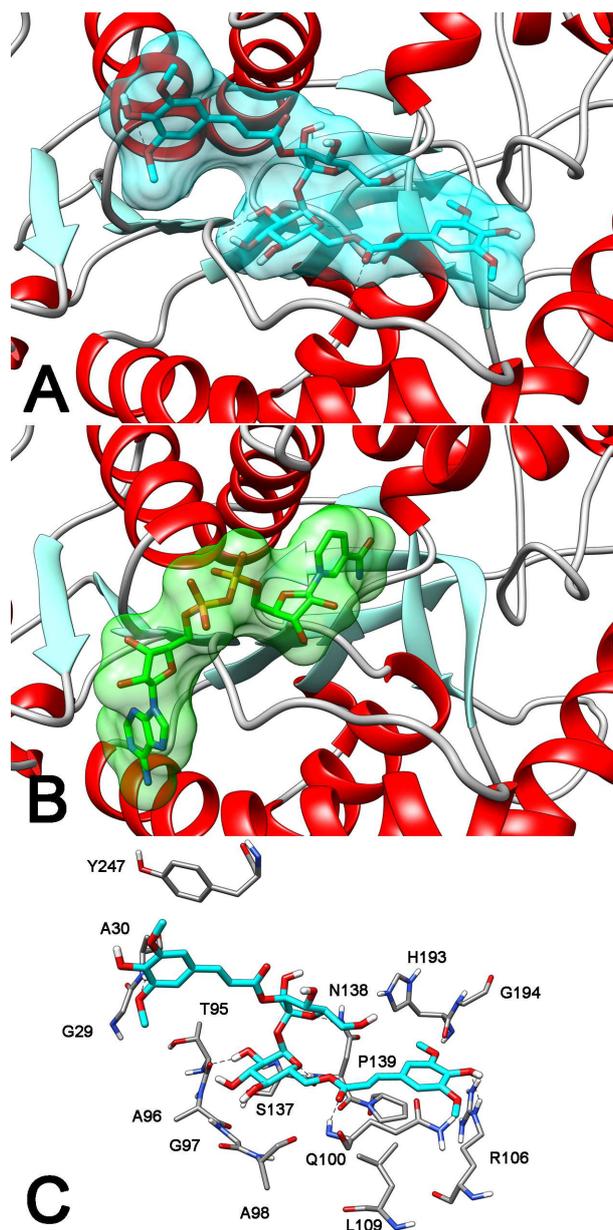
Figure 2. Analysis of the minimized average structure of compound **11** bound to *h*LDH5 (Cluster 01). Comparison between the (A) putative binding pose of the ligand (cyan) in the binding site and (B) the binding disposition of NADH (green) into *h*LDH5 (4M49 PDB code); (C) view of the most relevant ligand-receptor interactions of the **11**-*h*LDH5 complex. Hydrogen bonds are represented as black dashed lines.

Table 1. ^{1}H and ^{13}C NMR Data of Compounds **1-4** [a]

| position	1 δ_H	1 δ_C	2 δ_H	2 δ_C	3 δ_H	3 δ_C	4 δ_H	4 δ_C
2		158.0		158.4		158.0		158.0
3		134.0		134.1		134.7		134.0
4		179.0		179.0		179.3		179.0
5		163.1		163.2		163.0		163.1
6	6.13 d (2.0)	99.6	6.13 d (2.0)	99.3	6.14 d (1.8)	99.3	6.13 d (2.0)	99.5
7		165.5		165.3		165.0		165.0
8	6.07 d (2.0)	94.5	6.07 d (2.0)	94.0	6.09 d (1.8)	94.5	6.14 d (2.0)	94.2
9		158.0		157.7		157.7		157.8
10		105.3		105.7		105.0		105.0
1'		123.6		123.5		123.8		123.6
2'	7.51 d (2.0)	117.2	7.56 d (2.0)	117.2	7.59 d (2.0)	117.2	7.58 d (2.0)	117.2
3'		145.8		146.2		146.0		146.1
4'		149.6		149.4		149.0		149.1
5'	6.84 d (8.0)	116.0	6.88 d (8.0)	115.6	6.84 d (8.0)	116.0	6.86 d (8.0)	115.7
6'	7.52 dd (8.0, 2.0)	123.4	7.60 dd (8.0, 2.0)	123.0	7.57 dd (8.0, 2.0)	122.6	7.57 dd (8.0, 2.0)	122.8
glc-1	5.60 d (7.5)	100.5	5.57 d (7.8)	100.1	5.61 d (8.0)	100.0	5.57 d (7.8)	100.1
2	3.72 dd (9.0, 7.5)	77.2	3.75 dd (9.5, 7.8)	77.8	3.78 dd (9.5, 8.0)	77.7	3.73 dd (9.5, 7.8)	77.3
3	3.60 t (9.0)	78.7	3.58 t (9.5)	78.4	3.60 t (9.5)	78.3	3.57 t (9.5)	78.1
4	3.29 t (9.0)	71.8	3.25 t (9.5)	71.8	3.28 t (9.5)	71.6	3.28 t (9.5)	71.8
5	3.35 m	77.0	3.34[b]	76.9	3.33[b]	76.8	3.33[b]	76.8
6a	3.82 dd (12.0, 3.0)	68.3	3.83 dd (12.0, 3.5)	68.0	3.84 dd (12.0, 3.5)	68.0	3.83 dd (12.0, 3.0)	68.0
6b	3.42 dd (12.0, 4.5)		3.40 dd (12.0, 5.0)		3.40 dd (12.0, 5.0)		3.41 dd (12.0, 5.0)	
rha-1	4.50 d (1.8)	102.1	4.50 d (2.0)	101.9	4.52 d (1.8)	101.8	4.51 d (1.8)	101.6
2	3.60 dd (3.0, 1.8)	72.0	3.60 dd (3.0, 2.0)	71.7	3.62 dd (3.0, 1.8)	71.8	3.60 dd (3.0, 1.8)	71.8
3	3.49 dd (9.0, 3.0)	72.0	3.48 dd (9.0, 3.0)	72.0	3.52 dd (9.0, 3.0)	72.0	3.50 dd (9.0, 3.0)	72.0
4	3.25 t (9.0)	74.0	3.24 t (9.0)	74.0	3.22 t (9.0)	73.7	3.24 t (9.0)	73.5
5	3.44 m	69.5	3.43 m	69.6	3.45 m	69.4	3.43 m	69.3
6	1.06 d (6.5)	17.7	1.09 d (6.5)	17.4	1.05 d (6.0)	17.5	1.10 d (6.5)	17.0
api-1	5.52 d (3.0)	109.5	5.52 d (3.0)	109.0	5.53 d (2.5)	109.0	5.51 d (3.0)	108.8
2	3.94 br s	78.1	3.90 br s	78.0	3.94 br s	77.5	3.94 br s	78.1
3		79.6		79.3		80.4		79.6
4a	4.39 d (10.0)	75.2	4.41 d (10.0)	75.5	4.38 d (10.0)	75.0	4.30 d (11.0)	75.2
4b	3.74 d (10.0)		3.74 d (10.0)		3.74 d (10.0)		3.73 d (11.0)	
5a	4.66 d (10.5)	69.5	4.53 d (11.0)	69.5	4.53 d (11.0)	69.4	4.48 d (10.5)	69.4
5b	4.45 (10.5)		4.37 (11.0)		4.36 (11.0)		4.35 (10.5)	
acyl-1		131.0		126.2		127.0		126.8
2	7.76 dd (7.5, 1.5)	130.1	6.65 s	106.5	6.96 d (2.0)	110.5	7.23 d (7.8)	130.9
3	7.31 t (7.5)	129.3		149.3		149.2	6.77 d (7.8)	116.6
4	7.46 t (7.5)	134.0		139.1		146.7		160.6
5	7.31 t (7.5)	129.3		149.3	6.79 d (7.8)	115.8	6.77 d (7.8)	116.6
6	7.76 dd (7.5, 1.5)	130.1	6.65 s	106.5	6.83 dd (7.8, 2.0)	123.9	7.23 d (7.8)	130.9
α			6.12 d (16.0)	115.2	6.13 d (16.0)	114.4	6.12 d (15.8)	114.2
β			7.26 d (16.0)	146.3	7.30 d (16.0)	146.0	7.35 d (15.8)	147.0
COO		168.0		169.1		168.9		168.8
OMe			3.86 s	56.5	3.87 s	55.9		

*a*Spectra were run in methanol-d_4 at 600 MHz (^{1}H) and 150 MHz (^{13}C). J values are in parentheses and reported in Hz; chemical shifts are given in ppm; assignments were confirmed by COSY, 1D-TOCSY, HSQC, and HMBC experiments. *b*Overlapped signal.

Table 2. ^{1}H and ^{13}C NMR Data of Compounds **5-7** [a]

position	δH (5)	δC (5)	δH (6)	δC (6)	position	δH (7)	δC (7)
glc-1	5.48 d (3.0)	93.2	5.47 d (3.0)	92.7	1		35.7
2	3.63 dd (9.5, 3.0)	72.4	3.63 dd (9.0, 3.0)	72.3	2a	1.56 dd (14.0, 8.0)	47.6
3	3.92 t (9.5)	85.5	3.91 t (9.0)	85.2	2b	1.22 dd (14.0, 3.0)	
4	3.38 t (9.5)	69.7	3.47 t (9.0)	69.7	3	3.75 m	64.5
5	4.15 m	71.0	3.92 m	73.6	4a	2.27 dd (13.0, 3.5)	41.3
6a	4.51 dd (12.0, 3.5)	65.6	3.78 dd (12.0, 3.0)	62.1	4b	1.63 dd (13.0, 9.0)	
6b	4.14 dd (12.0, 5.5)		3.65 dd (12.0, 4.5)		5		68.6
CO<u>CH</u>₃	2.13 s	21.4			6		71.3
<u>CO</u>CH₃		171.0			7	5.97 d (16.0)	127.8
glc 2-1	4.54 d (7.8)	104.7	4.53 d (8.0)	104.9	8	5.74 dd (16.0, 5.5)	136.9
2	3.29 dd (9.0, 7.8)	75.0	3.29 dd (9.0, 8.0)	75.2	9	4.40 dq (6.5)	77.0
3	3.40 t (9.0)	77.9	3.41 t (9.0)	77.8	10	1.29 d (6.0)	21.0
4	3.31 t (9.0)	71.3	3.31 t (9.0)	71.3	11	1.15 s	29.6
5	3.43 m	77.0	3.36 m	77.8	12	0.98 s	25.0
6a	3.91 dd (12.0, 3.0)	62.0	3.91 dd (12.0, 3.0)	62.0	13	1.20 s	19.9
6b	3.76 dd (12.0, 5.0)		3.78 dd (12.0, 4.5)		Glc 1	4.34 d (7.8)	102.3
fru-1	3.65 d (12.0)	63.6	3.67 d (12.0)	64.0	2	3.19 dd (9.5, 7.8)	75.0
2		105.5		105.1	3	3.25 t (9.5)	77.5
3	4.16 d (8.0)	77.8	4.16 d (8.0)	78.5	4	3.33 t (9.5)	71.2
4	4.14 t (8.0)	77.0	4.13 t (8.0)	76.8	5	3.35 m	77.5
5	4.16 m	80.9	4.11 m	80.3	6a	3.96 dd (12.0, 3.5)	68.0
6a	4.65 dd (11.5, 6.0)	67.6	4.65 dd (12.0, 6.5)	67.2	6b	3.58 dd (12.0, 5.0)	
6b	4.60 dd (11.5, 4.0)		4.60 dd (12.0, 4.0)		Api 1	4.98 d (3.0)	110.0
benzoyl-1'		131.0		130.6	2	3.91 br s	77.5
2'/6	8.06 dd (7.5, 1.5)	130.6	8.07 dd (7.5, 1.5)	130.4	3		80.4
3/5	7.50 t (7.5)	129.7	7.51 t (7.5)	129.0	4a	3.98 d (11.0)	74.5
4	7.63 t (7.5)	133.8	7.63 t (7.5)	133.5	4b	3.77 d (11.0)	
COO		168.0		167.5	5a	3.75 d (10.5)	64.5
					5b	3.58 d (10.5)	

[a] Spectra were run in methanol-d_4 at 600 MHz (^{1}H) and 150 MHz (^{13}C). J values are in parentheses and reported in Hz; chemical shifts are given in ppm; assignments were confirmed by COSY, 1D-TOCSY, HSQC, and HMBC experiments.

Table 3. ^{1}H and ^{13}C-NMR Data of Compounds **8-10** Sugar Moieties (CD$_3$OD, 600 MHz, J in Hz) [a]

position	8		9		10	
	δ_H	δ_C	δ_H	δ_C	δ_H	δ_C
glc-1	4.44 d (7.8)	103.8	4.34 d (8.0)	104.1	4.42 d (8.0)	103.5
2	3.23 dd (9.0, 7.8)	75.0	3.24 dd (9.5, 8.0)	75.1	3.23 dd (9.5, 8.0)	75.2
3	3.37 t (9.0)	77.0	3.37 t (9.5)	77.6	3.36 t (9.5)	77.2
4	3.35 t (9.0)	70.5	3.30 t (9.5)	71.0	3.32[b]	70.5
5	3.26 m	76.3	3.28 m	77.5	3.32[b]	77.1
6a	3.80 dd (12.0, 3.0)	61.6	3.92 dd (12.0, 2.5)	62.5	3.92 dd (12.0, 2.5)	61.7
6b	3.69 dd (12.0, 4.5)		3.69 dd (12.0, 5.0)		3.69 dd (12.0, 5.0)	
fuc-1	5.47 d (8.0)	94.5	5.49 d (7.8)	94.5	5.41 d (7.8)	93.8
2	3.73 dd (9.0, 8.0)	74.0	3.97 dd (9.0, 7.8)	72.7	3.65 dd (9.0, 7.8)	75.7
3	3.89 dd (9.0, 4.0)	79.9	4.05 dd (9.0, 4.0)	79.5	3.86 dd (9.0, 4.0)	85.0
4	5.30 dd (4.0, 2.5)	73.8	5.41 dd (4.0, 2.5)	75.0	3.66 dd (4.0, 2.5)	70.6
5	3.87 m	70.7	3.85 m	72.0	3.74 m	71.0
6	1.08 d (6.0)	16.4	1.15 d (6.0)	16.0	1.16 d (6.0)	16.4
COCH$_3$		172.8		172.0		
COCH$_3$	2.16 s	20.0	2.18 s	20.4		
rha-1	5.10 d (1.8)	102.1	5.51 d (1.8)	101.2	5.47 d (1.8)	99.5
2	3.95 dd (3.0, 1.8)	70.7	3.97 dd (3.0, 1.8)	71.5	3.95 dd (3.0, 1.8)	71.5
3	3.66 dd (9.0, 3.0)	71.0	3.90 dd (9.0, 3.0)	71.0	3.99 dd (9.0, 3.0)	70.9
4	3.37 t (9.0)	72.8	3.54 t (9.0)	84.0	3.52 t (9.0)	84.0
5	3.70 m	70.3	3.86 m	68.3	3.83 m	69.0
6	1.24 d (6.5)	16.4	1.32 d (6.5)	18.0	1.30 d (6.5)	18.0
xyl-1			4.51 d (7.5)	106.0	4.54 d (7.5)	104.5
2			3.16 dd (9.0, 7.5)	75.0	3.23 dd (9.0, 7.5)	74.7
3			3.49 t (9.0)	76.0	3.29 t (9.0)	76.6
4			3.37 m	77.6	3.36 m	77.0
5a			4.04 dd (11.0, 2.5)	64.7	4.04 dd (11.0, 2.5)	64.5
5b			3.31 dd (11.0, 5.0)		3.28 dd (11.0, 5.0)	
gal-1			4.39 d (7.5)	104.1	4.45 d (7.8)	105.7
2			3.59 dd (8.0, 7.5)	72.0	3.53 dd (9.0, 7.8)	73.6
3			3.52 dd (8.0, 4.0)	74.6	3.48 dd (9.0, 3.5)	75.4
4			3.83 dd (4.0, 2.5)	70.0	3.84 dd (3.5, 2.0)	70.7
5			3.64 m	75.9	3.73 m	76.0
6a			3.76 dd (11.5, 2.5)	62.3	3.86 dd (11.0, 2.5)	61.5
6b			3.69 dd (11.5, 4.5)		3.65 dd (11.0, 5.0)	
api-1	5.14 d (3.0)	112.0				
2	3.97 br s	77.0				
3		80.6				
4a	3.97 d (10.0)	74.6				
4b	3.74 d (10.0)					
5	3.52 br s	64.0				
glc-1			4.51 d (8.0)	105.2	4.42 d (8.0)	103.0
2			3.24 dd (9.0, 8.0)	75.1	3.24 dd (9.0, 8.0)	75.1
3			3.37 t (9.0)	77.6	3.37 t (9.0)	77.6
4			3.23 t (9.0)	71.0	3.30 t (9.0)	70.0
5			3.31 m	76.0	3.31 m	76.0
6a			3.92 dd (12.0, 3.0)	62.8	3.83 dd (12.0, 3.0)	62.0
6b			3.62 dd (12.0, 4.5)		3.70 dd (12.0, 4.5)	

[a]Spectra were run in methanol-d_4 at 600 MHz (^{1}H) and 150 MHz (^{13}C). J values are in parentheses and reported in Hz; chemical shifts are given in ppm; assignments were confirmed by COSY, 1D-TOCSY, HSQC, and HMBC experiments. [b]Overlapped signal.

Table 4. hLDH5 Inhibition Potencies

compound	hLDH5[a] (IC$_{50}$, μM)
1	> 500
2	>500
3	>500
4	>500
5	>500
6	>500
8	>500
11	90.4 ± 4.4
12	190.7 ± 21.8
13	>500
14	>500
galloflavin	102.4 ± 15.0

[a]Values are reported as the means ± SD of three or more independent experiments.

Table 5. MM-PBSA Resulting Values for the Ten Different *h*LDH5-Compound **11** Complexes [a,b]

| | MM-PBSA evaluation | | | | |
	VDW	EEL	EPB	ENP	ΔPBSA
cluster 01	-62.0	-53.1	89.5	-6.6	-32.2
cluster 02	-76.4	-53.2	113.1	-7.4	-23.9
cluster 03	-60.8	-39.5	82.8	-5.9	-23.4
cluster 04	-73.2	-46.1	105.0	-7.0	-21.3
cluster 05	-56.4	-40.5	83.0	-6.4	-20.3
cluster 06	-64.2	-45.5	94.5	-6.9	-22.1
cluster 07	-51.4	-31.5	69.6	-5.6	-18.9
cluster 08	-49.4	-37.6	78.5	-5.8	-14.3
cluster 09	-59.4	-28.6	75.8	-7.1	-19.3
cluster 10	-39.4	-29.5	60.4	-4.8	-13.3

[a]ΔPBSA is the total amount of the electrostatic (EEL), van der Waals (VDW), polar (EPB) and non-polar (ENP) solvation free energy. [b]Data are expressed as kcal/mol.